

# Removal of a cationic dye, methylene blue, from water by cotton stem ash as a novel adsorbent

Rakesh Kumar Ghosh<sup>1,2\*</sup>, D. Damodar Reddy<sup>1</sup>, Deb Prasad Ray<sup>2</sup>



<sup>1</sup>Central Tobacco Research Institute, Rajahmundry-533105, Andhra Pradesh, India;

<sup>2</sup>National Institute of Research on Jute and Allied Fibre Technology, Kolkata-700040, India;

**E-mail:** iarirakesh@gmail.com

Paper No.

Received:

Accepted:

## Abstract

In search of an efficient and no-cost adsorbent for removal of methylene blue (MB) from water, cotton stem ash (CSA) was evaluated. The effect of process variables, namely, contact time, solution pH and adsorbent dose on adsorption of MB onto CSA were investigated. The adsorption kinetics and mechanism were tested with pseudo-first order and pseudo-second order model, and with intraparticle diffusion model, respectively. Based on error analysis (chi-square and percent sum of error) the suitability order of adsorption isotherms was Langmuir>Temkin>Freundlich>Jovanoic. The maximum adsorption capacity of CSA was 20.42 mg g<sup>-1</sup>. The feasibility parameter and free energy change were also calculated. The present study demonstrated that the CSA could be used as a potential, efficient, low-cost, and easily available adsorbent for the treatment of MB containing industrial wastewater.

## Highlights

- For the first time, this study reported CSA as a potential, efficient and no-cost adsorbent for removal of methylene blue (MB) from water.
- Effects of different process variables were investigated and optimized.
- The maximum MB adsorption capacity of CSA was 20.42 mg g<sup>-1</sup>.

**Keywords:** Cotton stem ash, methylene blue, adsorption kinetics, mechanism, isotherm

Pollution of water bodies with synthetic dye stuff is a burning environmental issue close to the globe. Wastewater from textile, paper, leather and other related industries contains 5-10% residues of synthetic dyes and are often released untreated into the environment, especially in developing nations (Rafatullah *et al.* 2010; Feng *et al.* 2012). These synthetic dyes have long persistence owing to molecular stability and complexity, which result in low or no degradation by natural biotic and abiotic processes (Arabi and Sohrabi, 2014). Hence, colored effluents, if not treated before disposal to the environment, can contaminate natural water bodies. Synthetic dyes may adversely affect aquatic life, water quality and esthetic value of receiving

water systems, and therefore present a severe environmental problem (Bharathi and Ramesh, 2013). Therefore, removal of dyes from industrial effluents before discharging into the environment is extremely important. Though several technologies are available to treat dye contaminated water, the adsorption method is widely used because of its efficiency and practical feasibility (Yagub *et al.* 2012). Nevertheless, the cost of adsorbent controls the political economy of an adsorption technique. That is why, though activated carbon is a well known adsorptive material, its high cost often restricts its application for wastewater treatment in developing countries. This has prompted research into renewable alternative easily available, effective



and low-cost adsorbents (Annadurai *et al.*, 2002; Hameed *et al.* 2008; Reddy *et al.* 2012). However, till this study, cotton stem ash (CSA) remained unexplored as a potential adsorbent for treating colored wastewater.

Cotton (*Gossypium* spp.), one of the leading cash crop of the world, is widely grown in USA, China, India, Australia, Africa, etc. Cotton cultivation generates nearly 6.7 tonnes residue (dry weight basis) per hectare per crop season (Lal, 2005). In India, nearly 11.8 million tonnes of cotton stalk biomass is being generated every year (Pathak, 2006). This highly lignocellulosic biomass has no or limited application either for manuring or for cattle feed. Hence, the general practice is open burning of cotton stem biomass, which generates CSA with no or limited economic uses. The obvious advantages of using the CSA as adsorbents for treatment of dye-bearing wastewater include easy availability, global abundance and low cost.

The present study aims to evaluate methylene blue (MB), a basic dye, adsorption capacity of CSA and the feasibility of adsorption process. The CSA was characterized on the basis of physicochemical parameters (pH, electrical conductivity and total organic carbon), surface charge in terms of pH zero point charge ( $\text{pH}_{\text{zpc}}$ ) and functional group analysis. Effect of different process variables, namely, contact time, solution pH and the dose of adsorbent, were investigated. The kinetics and mechanism of adsorption were studied with pseudo-first order and pseudo-second order, and intraparticle diffusion model, respectively. To understand the equilibrium adsorption, four mathematical models, Freundlich, Langmuir, Temkin and Jovanoic isotherm, were examined. Feasibility of adsorption process and the free energy change in adsorption were also investigated. Chi-square and percent sum of error analysis were carried out to identify the error associated with different models and these error analysis was utilized to choose the best model, describing the likely mechanism involved.

## Materials and Methods

### *Adsorbent and its characterization*

Cotton crop residues were collected from local farmer's field near the Central Tobacco Research Institute, Rajahmundry, Andhra Pradesh, India

(16.98°N 81.78°E). These residues were cleaned thoroughly to get rid of the surface adhered soil and dried. About 10 kg of dried cotton stems were incinerated in open air to simulate the pattern adopted by local farmers, i.e. burning of stems kept in heaps and it required almost 30 min for complete combustion. After burning 10 kg of cotton stem biomass yielded 0.853 kg (91.47% weight loss) cotton stem ash (CSA). The CSA was sieved (1 mm), stored and used in different experiment. The CSA was analyzed for organic carbon (OC) using a TOC analyzer (Elementar, Vario TOC select, Gernamy), pH (Systronics, Model 361, India) and electrical conductivity (EC) (Elico, Model CM 82T, India). The surface charge of CSA was determined by measuring pH of zero point charge ( $\text{pH}_{\text{zpc}}$ ) by the potentiometric mass titration method (Foil and Villaescusa, 2009). The functional groups of CSA were determined by the Bruker ALPHA, Fourier transform infrared using attenuated total reflectance (FTIR/ATR) system. Samples were scanned (resolution-  $4\text{cm}^{-1}$ ) in the region of  $4000\text{--}400\text{ cm}^{-1}$ . The specific surface area was determined by Weng & Pan's (2006) method.

### *Dye and other reagents*

Methylene blue (MB) (basic blue 9; molecular weight  $373.91\text{ g mol}^{-1}$  and  $\lambda_{\text{max}} = 665\text{ nm}$ ) with analytical grade purity was procured from the Qualigens Fine Chemicals (Mumbai, India). The MB concentration in aqueous solution was determined by using UV-Vis spectrophotometry (Systronics, Model 2202, India) at a wavelength of maximum absorbance ( $\lambda_{\text{max}}$ ) of 665 nm. The molecular stability of MB was confirmed over the experimental solution pH range (2-12) as the  $\lambda_{\text{max}}$  (665 nm) remained unchanged. All reagents used in experiments were analytical grade and procured from Merck (Mumbai, India). Deionized water (pH- 7.01) was used throughout the experimental procedures.

### *Adsorption experiments*

Adsorption experiments were carried out by a batch adsorption method with an orbital shaker Rotary Flask Shaker, Optics Technology, India). The effect of different process variables, namely, contact time (0-300 min), initial solution pH (ranging from 2-8, acidic or alkaline pH values were obtained by adding HCl or NaOH solutions) and adsorbent dose

(2.5-25 g L<sup>-1</sup>) were investigated. The effect of contact time and initial solution pH were simultaneously investigated by agitating 0.5 g CSA with 50 mL MB solution (concentration – 50 mg L<sup>-1</sup>) of different pH values (2-8) at 150 r.p.m over a period of 300 min. A set of three flasks each were withdrawn at different time intervals (15, 30, 45, 60, 120, 180, 240 and 300 min) over the studied pH range (2, 4, 6 and 8). The resulting suspensions were centrifuged (Remi, Model-PR 24, Mumbai, India) at 5000 r.p.m. for 10 min and the MB concentration in the supernatant was estimated by measuring absorbance with UV-VIS spectrophotometer at  $\lambda_{\max}$  of 665 nm. The amount of dye adsorbed at any time  $t$ ,  $q_t$  (mg g<sup>-1</sup>), at the equilibrium time  $q_e$  (mg g<sup>-1</sup>) and percentage dye removal were calculated as:

$$q_t = (C_i - C_t)V/W \quad (1)$$

$$q_e = (C_i - C_e)V/W \quad (2)$$

$$\% \text{ Dye adsorption} = 100(C_i - C_t)/C_i \quad (3)$$

where,  $C_i$ ,  $C_t$  and  $C_e$  are the MB concentrations (mg L<sup>-1</sup>) at initial time ( $t=0$ ), at any time and at equilibrium, respectively.  $V$  is the volume of the solution (L) and  $W$  is the amount of adsorbent (g).

The effect of adsorbent dose was investigated by equilibrating different quantities of CSA (2.5, 5, 10, 15, 20 and 25 g L<sup>-1</sup>) with 50 mL MB solution (pH 7.01) of known concentration (50 mg L<sup>-1</sup>) at 150 r.p.m for 180 min. Equilibrium adsorption experiments were carried out by agitating 0.1 g of CSA with 50 mL MB solution (pH 7.01) of different concentration (25, 50, 75, 100, 154, 200 and 269 mg L<sup>-1</sup>) at 150 r.p.m. over a time period of 180 min.

All experiments were carried out in triplicate and the relative standard deviation was calculated. Only mean values are reported (with relative standard deviation < 10 %) for ease of presentation. Adsorbate and adsorbent blanks were carried out simultaneously in all experiments as control to monitor interference. All batch adsorption studies were carried out at room temperature (27±1 °C).

### *Kinetic models and equilibrium isotherms*

The MB adsorption kinetics onto CSA was investigated by fitting the kinetic data (obtained under different pH ranging from 2 to 8 of the MB solution with 50 mg L<sup>-1</sup> concentration) to the pseudo-first-order (Lagergren and Svenska, 1898),

pseudo-second order (Ho and McKay, 1998) and intra-particle diffusion model (Weber and Morris, 1963). These kinetic models can be expressed in linear form as:

$$\log (q_e - q_t) = \log q_e - (k_1/2.303) t \quad (4)$$

$$t/q_t = 1/(k_2 q_e^2) + (1/q_e) t \quad (5)$$

$$q_t = k_{id} t^{0.5} + C \quad (6)$$

where  $k_1$ ,  $k_2$  and  $k_{id}$  are the rate constants of pseudo-first order, pseudo-second order and intraparticle diffusion rate constants, respectively, in (min<sup>-1</sup>), (g mg<sup>-1</sup> min<sup>-1</sup>) and (mg g<sup>-1</sup> min<sup>-0.5</sup>),  $C$  (mg g<sup>-1</sup>) reflects the boundary layer effect in intraparticle diffusion.

In order to obtain best equilibrium model, the equilibrium adsorption data were tested by four isotherm models, namely, Freundlich (Freundlich, 1904), Langmuir (Langmuir, 1918), Temkin (Temkin and Pyzhev, 1940) and Jovanoic (Jovanoic, 1969) isotherm. These models can be expressed in linear form as:

$$\log q_e = \log K_f + (1/n) \log C_e \quad (7)$$

$$C_e/q_e = 1/kb + C_e/b \quad (8)$$

$$q_e = \alpha + \beta \ln C_e \quad (9)$$

$$\ln q_e = \ln q_m + K_j C_e \quad (10)$$

where  $K_f$  (mg g<sup>-1</sup>) and  $1/n$  are Freundlich constants indicating capacity and heterogeneity factor, respectively,  $b$  (mg g<sup>-1</sup>) and  $k$  (L mg<sup>-1</sup>) are the Langmuir maximum adsorption capacity and the Langmuir bonding energy coefficient, respectively,  $\alpha$  and  $\beta$  are Temkin constants resending adsorption capacity and retention intensity, respectively,  $q_m$  (mg g<sup>-1</sup>) and  $K_j$  (L mg<sup>-1</sup>) are Jovanoic constants related to adsorption maxima and energy of adsorption, respectively.

### *Statistical analysis*

The best-fit isotherm model was selected on the basis of error analysis by Chi-square ( $\chi^2$ ) test and per cent sum of error (SE). Chi-square ( $\chi^2$ ) and per cent sum of error (SE) are calculated by the following equations as:

$$\chi^2 = (\sum (q_{e,exp} - q_{e,cal})^2) / q_{e,cal} \quad (11)$$

$$SE (\%) = 100 \sum (q_{e,exp} - q_{e,cal}) / q_{e,exp} / (N-1) \quad (12)$$

where,  $q_{e,exp}$  ( $\text{mg g}^{-1}$ ) and  $q_{e,cal}$  ( $\text{mg g}^{-1}$ ) are the amount of dye adsorbed at equilibrium from experiment and mathematical model, respectively,  $N$  is the number of observations.

## Results and Discussion

### Characterization of CSA

Physicochemical analysis revealed that organic carbon, electrical conductivity and pH of CSA were 5.64 %, 8.53  $\text{dS m}^{-1}$  and 11.2, respectively. CSA's surface charge was estimated by measuring the  $\text{pH}_{zpc}$  (Figure 1). The  $\text{pH}_{zpc}$  of CSA was 10.62. Figure 2 shows presence various functional groups onto CSA, which could be helpful to understand the MB adsorption process. Band at  $1034 \text{ cm}^{-1}$  coupled with bands around  $700\text{-}800 \text{ cm}^{-1}$  represented Si-O asymmetric and symmetric stretching vibrations, respectively. Bands near  $500\text{-}650 \text{ cm}^{-1}$  represented the silicate backbone of CSA (Sarkar *et al.* 2006). A strong band at  $1437 \text{ cm}^{-1}$  coupled with a band at  $872 \text{ cm}^{-1}$  showed asymmetric stretching and out-of-plane bending vibration, respectively, of carbonates ( $\text{CO}_3^{2-}$ ). Ionization of these polar functional groups may significantly influence the absorption of the basic MB in aqueous medium. The specific surface area of CSA was  $23.19 \text{ m}^2 \text{ g}^{-1}$ .

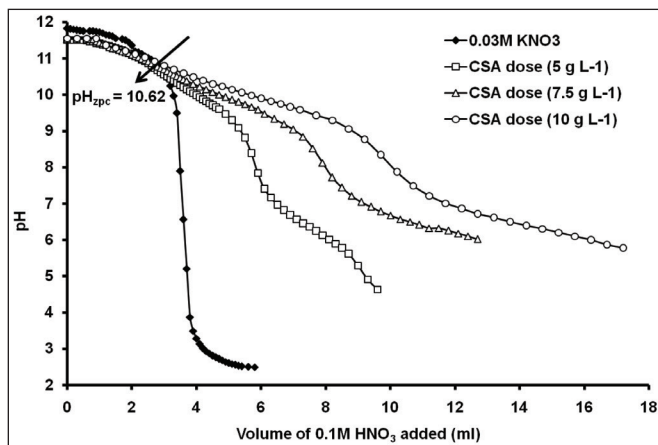


Fig. 1 Surface charge ( $\text{pHzpc}$ ) determination of CSA

of 180 min, the % MB adsorption increased from 56.4% to 84.3% ( $q_t$  increased from  $2.82$  to  $4.22 \text{ mg g}^{-1}$ ) with a rise in initial solution pH from 2 to 8. This can be explained by the  $\text{pHzpc}$  of CSA, ionization of the CSA and pH of the final solution. MB exists as a cation in aqueous medium and gets adsorbed

### Effect of contact time and pH

Figure 3 depicts the effect of contact time and initial solution pH on the % dye adsorption by CSA. MB adsorption was fast at the initial process of adsorption. About 39.8-54.2 % of MB solution concentration were removed within 15 min of adsorption process. It could be attributed due to the large availability of adsorption sites of CSA. The very moment, these sites came in contact with the MB solution, very fast diffusion of MB molecules might have occurred from bulk dye solution to the adsorption sites of CSA (Yagub *et al.* 2012; Reddy *et al.* 2012). Afterwards, the rate of adsorption decreased with increase in contact time, and after 180 min the % dye adsorption values marginally increased by less than 4% (up to 300 min). These increments in MB removal were marginal at the cost of 1.67 times higher contact time. As shown in Figure 3, the % MB adsorption were different for solution of different initial pH values, however, the state of equilibrium were reached within 180 min, in all conditions. Thus, 180 min was selected as an optimum contact time for attaining equilibrium in all other experiments.

Figure 3 also shows the effect pH dynamic on the adsorption of MB onto CSA. At equilibrium time

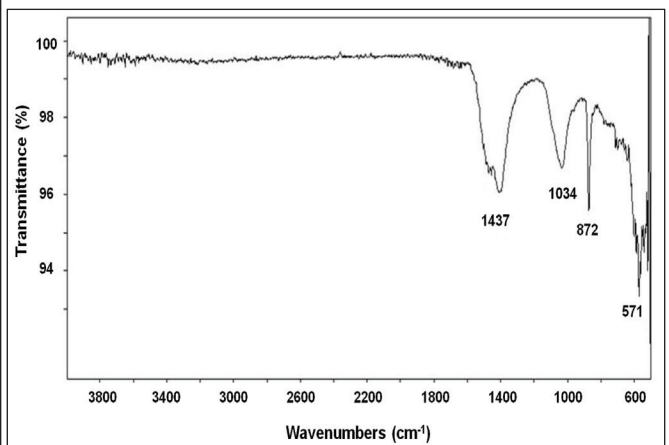


Fig. 2: FTIR spectral analysis of CSA representing various functional groups.

on the negatively charged sites of the adsorbents. The adsorbent acquires negatively charged sites only when the pH of the solution is higher than the adsorbent's  $\text{pH}_{zpc}$  (Hameed *et al.* 2008; Arabi and Sohrabi, 2014). In the present case, the pH and  $\text{pH}_{zpc}$  of CSA were 11.2 and 10.62. Figure 3 shows

that the addition of CSA resulted in an increase in final solution pH. The pH enhancement was lower in solution with initial pH 2 as compared with other solutions. Nevertheless, at the equilibrium time of 180 min, the final solution pH were 10.8, 11.33, 11.36 and 11.51 for initial solution pH of 2, 4, 6 and 8, respectively. These final solution pH values were higher than the  $pH_{zpc}$  (10.62) of the CSA and resulted in development of negatively charged sites onto the CSA surface by ionization of functional groups. The higher the final solution pH as compared to  $pH_{zpc}$  more will be the density of negative charges over CSA surface. This explained the higher adsorption of MB with increase in solution pH.

### Effect of CSA dose

Figure 4 depicts the effect of CSA dose on the removal of MB. MB adsorption increased from 43.1% to 79.1% with an increase in CSA dose from 2.5 to 10 g L<sup>-1</sup>, and thereafter % dye removal increased only by 20% with 150% higher amount of CSA. But, the quantity of MB adsorbed per unit mass of CSA ( $q_e$ ) decreased from 9.15 to 1.93 mg g<sup>-1</sup>. It could be explained as with increase in adsorbent's dose, the number of adsorbing sites increased and resulted in the higher percentage MB removal (Feng *et al.*

2012; Ghosh and Reddy, 2013). However, for a fixed volume of MB solution the number of unutilized adsorption sites increased with an increase in dose and resulted in less efficiency per unit mass of adsorbent. Hence, considering these facts, a CSA dose of 10 g L<sup>-1</sup> was considered as optimum dose.

### Kinetics and mechanism of adsorption

Figure 3 shows the results of kinetic experiments studied under different solution pH (2, 4, 6 and 8) with MB concentration of 50 mg L<sup>-1</sup> at 27±1 °C. The pseudo-first order and pseudo-second order models were tested to understand the adsorption kinetics. Table 1 represents different parameter values of these two kinetic models. Though the values of coefficient of determination for pseudo-first order ( $R^2 = 0.946-0.963$ ) and pseudo-second order ( $R^2 = 0.97-0.997$ ) were close, but the  $q_{e,exp}$  values were in close agreement with  $q_{e,cal}$  values from pseudo-second order model as compared to pseudo-first order kinetic model. Hence, the pseudo-second order model with higher  $R^2$  and better production values was selected as a best fit kinetic model. Similar observations were reported for some other adsorbents like pine leaves (Yagub *et al.* 2012), tobacco stem ash (Ghosh and Reddy, 2013) etc.

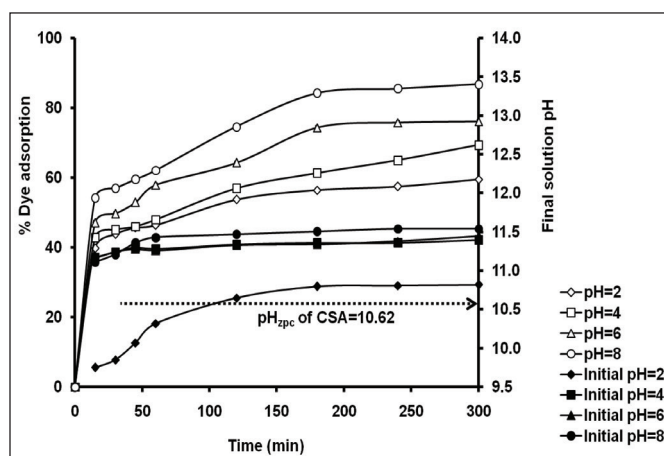


Fig. 3: Effect of contact time and initial solution pH on adsorption of MB onto CSA.

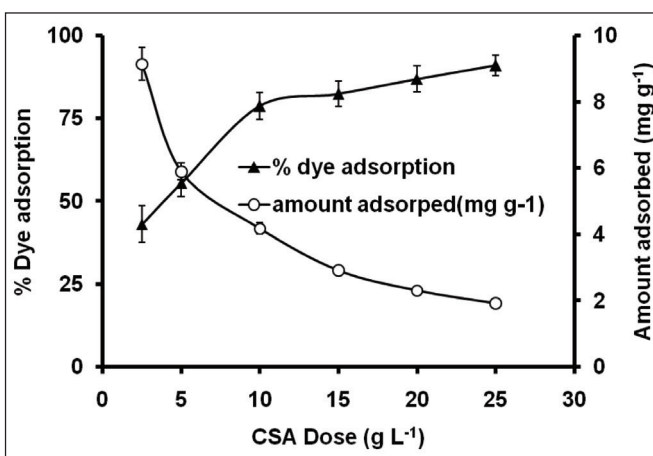


Fig. 4: Effect of adsorbent dose on adsorption of MB onto CSA.

The adsorption mechanism was investigated by fitting the kinetic data to intraparticle diffusion model (Figure 5). Figure 5 depicted that adsorption plots were not linear over the experimental time period, indicating multi-stage adsorption process (Reddy *et al.* 2008). The intraparticle diffusion rate constant ( $k_{id}$ ) and C (boundary layer thickness)

were determined from the slope and intercept of the linear regression line of  $q_t$  against  $time^{0.5}$  (Table 1). Intraparticle diffusion becomes the only rate-limiting step when the linear regression lines of  $q_t$  against  $time^{0.5}$  pass through the origin, indicating no film diffusion ( $C=0$ ). Figure 5 and Table 1 showed that though the linear regression

**Table 1:** Kinetic parameters for adsorption of MB onto CRA.

Adsorbent	pH	$q_{e,exp}$ ( $mg\ g^{-1}$ )	Kinetic models								
			Pseudo-first-order			Pseudo-second-order			Intraparticle diffusion		
			$k_1$ ( $min^{-1}$ )	$R^2$	$q_{e,cal}$ ( $mg\ g^{-1}$ )	$k_2$ ( $g\ mg^{-1}\ min^{-1}$ )	$R^2$	$q_{e,cal}$ ( $mg\ g^{-1}$ )	$K_{id}$	$C$ ( $mg\ g^{-1}$ )	$R^2$
CRA	2	2.820	0.0161	0.962	1.089	0.0284	0.997	2.976	0.087	1.681	0.986
	4	3.070	0.0138	0.963	1.358	0.0203	0.992	3.268	0.103	1.675	0.975
	6	3.716	0.0092	0.946	1.589	0.0138	0.970	3.953	0.142	1.744	0.983
	8	4.215	0.0092	0.963	1.928	0.0114	0.991	4.525	0.162	1.960	0.977

**Table 2:** Adsorption isotherm parameters for MB adsorption onto CRA.

Freundlich isotherm		Langmuir isotherm		Temkin isotherm		Jovanoic isotherm	
Parameter	Values	Parameter	Values	Parameter	Values	Parameter	Values
$K_f$ ( $mg\ g^{-1}$ )	1.14	$b$ ( $mg\ g^{-1}$ )	20.41	$\alpha$	8.773	$q$ ( $mg\ g^{-1}$ )	5.766
$1/n$	0.497	$k$ ( $L\ mg^{-1}$ )	0.0147	$\beta$	4.495	$K_j$ ( $L\ mg^{-1}$ )	0.005
$R^2$	0.975	$R^2$	0.997	$R^2$	0.993	$R^2$	0.759
$\chi^2$	0.347	$\chi^2$	0.05	$\chi^2$	0.113	$\chi^2$	2.684
SE (%)	7.117	SE (%)	2.888	SE (%)	3.918	SE (%)	21.87

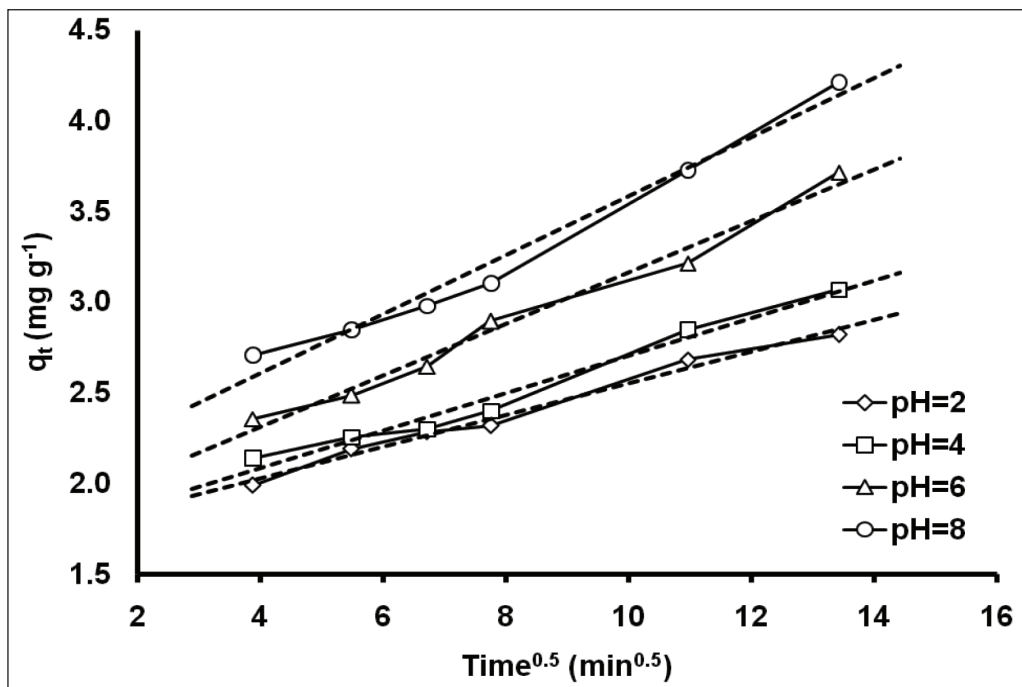


**Fig. 5:** Intraparticle diffusion model for adsorption of MB onto CSA.

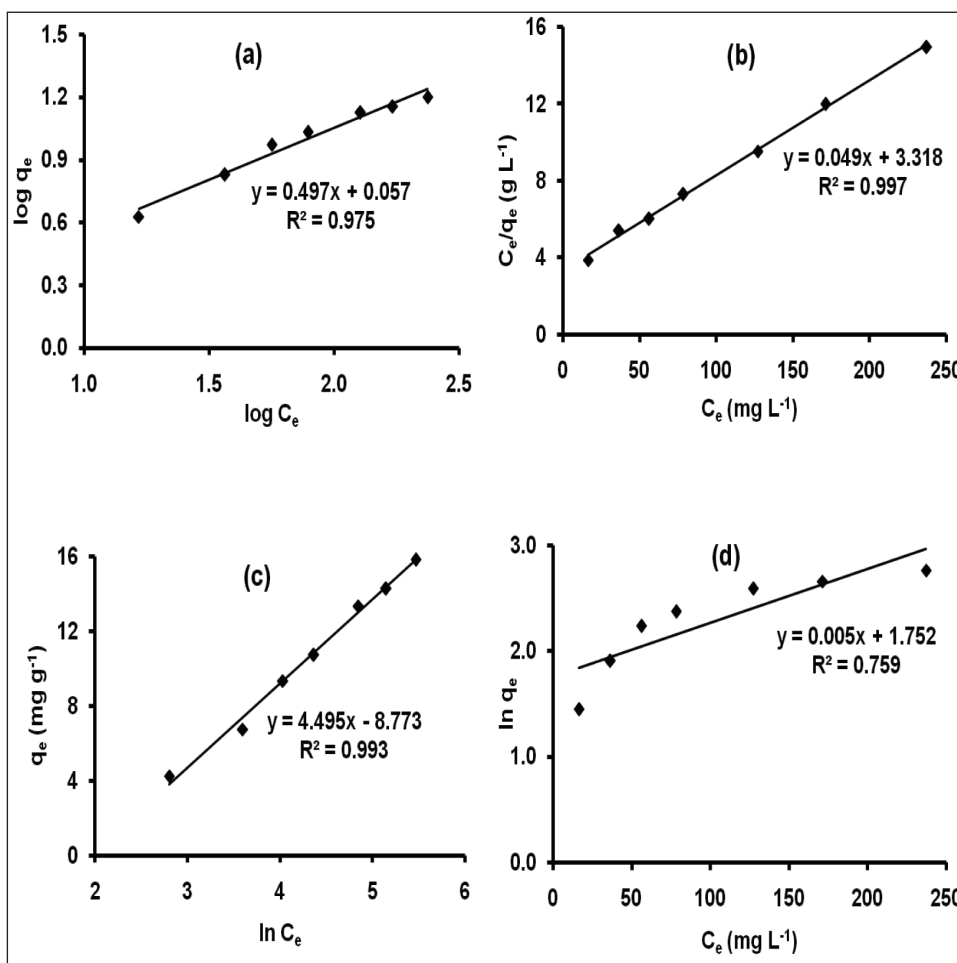


Fig. 6: Freundlich (a), Langmuir (b), Temkin (c) and Jovanoic (d) isotherms for equilibrium adsorption of MB onto CSA.

lines for intraparticle diffusion model had a high coefficient of determination ( $R^2=0.975-0.986$ ) but, the regression lines did not pass through the origin ( $C \neq 0$ ). These results indicated that intraparticle diffusion was not the sole mechanism of adsorption. Fast adsorption during initial stages could be predominantly controlled by film diffusion, while the slow adsorption at the later stages could be mainly governed by intraparticle diffusion (Hameed *et al.* 2008; Yagub *et al.* 2012; Ghosh and Reddy, 2014). Both  $K_{id}$  and  $C$  values increased with increase in solution pH, which also explained more MB adsorption at higher solution pH.

### Equilibrium study

Adsorption equilibrium was studied by evaluating Freundlich, Langmuir, Temkin and Jovanoic isotherms (Figure 6). Isotherm parameters were presented in the Table 2. Freundlich ( $R^2=0.975$ ), Langmuir ( $R^2=0.997$ ) and Temkin ( $R^2=0.993$ ) isotherms showed a better coefficient of determination as compared to

Jovanoic isotherm ( $R^2=0.759$ ) However, the best-fit isotherm was selected on the basis of error analysis. The predicted  $q_{e,cal}$  values were calculated from each isotherm and error was calculated in comparison with the actual  $q_{e,exp}$  values by determining the  $\chi^2$  and % SE. Langmuir isotherm with lowest  $\chi^2$  (0.05) and % SE (2.888) as compared to other models was selected as best-fit isotherm. However, the order of isotherm models for describing the equilibrium adsorption was Langmuir > Temkin > Freundlich > Jovanoic isotherm. The Langmuir monolayer adsorption capacity (b) of CSA was  $20.41 \text{ mg g}^{-1}$ . CSA was found to be better than many other earlier reported adsorbents for MB like bio-sludge ash ( $b=1.87 \text{ mg g}^{-1}$ , Weng and Pan, 2006), fly ash ( $b=4.48 \text{ mg g}^{-1}$ , Wang and Zhu, 2005), blast furnace sludge ( $b=6.4 \text{ mg g}^{-1}$ , Jain *et al.* 2003), rice husk ash ( $b=6.9 \text{ mg g}^{-1}$ , Sarkar and Bandyopadhyay, 2010), orange peel ( $b=18.6 \text{ mg g}^{-1}$ , Annadurai *et al.* 2002) etc. The feasibility of Langmuir monolayer adsorption was calculated by estimating the separation factor ( $R_L$ ) at



highest initial dye concentration for MB adsorption onto CSA by following equation:

$$R_L = 1/(1+kC_e) \quad (12)$$

$R_L$  value indicates either unfavorable ( $R_L > 1$ ), linear ( $R_L = 1$ ), favorable ( $0 < R_L < 1$ ) or irreversible ( $R_L = 0$ ) adsorption process. The  $R_L$  value for adsorption of MB onto CSA at highest initial dye concentration ( $269 \text{ mg L}^{-1}$ ) was 0.201 which indicated favorable ( $0 < R_L < 1$ ) process of adsorption. Further, the Gibb's free energy ( $\Delta G$ ) of MB adsorption onto CSA was determined from the Langmuir binding energy constant,  $k$  (Leechart *et al.* 2009). The  $k$  ( $\text{L mg}^{-1}$ ) was converted to  $K$  ( $\text{L mol}^{-1}$ ) by using the molecular weight of MB before calculating the free energy change as:

$$\Delta G = -RT \ln(K) \quad (13)$$

where  $\Delta G$  is the free energy change of adsorption ( $\text{kJ mol}^{-1}$ ),  $R$  is the universal gas constant ( $8.3145 \text{ J mol}^{-1} \text{ K}^{-1}$ ) and  $T$  is temperature (K). The  $\Delta G$  values for MB adsorption onto CSA was found to be  $-4.251 \text{ kJ mol}^{-1}$ , at  $27 \pm 1 \text{ }^\circ\text{C}$ . The negative value of  $\Delta G$  indicated a spontaneous and favorable adsorption of MB onto CSA.

## Conclusions

Cotton stem ash, an underutilized material, was tested as a novel adsorbent for removal of MB from aqueous medium. The effect of various process factors was investigated and optimized. The MB removal was optimized with  $10 \text{ g L}^{-1}$  dose of CSA and contact time was 180 min. The MB adsorption increased from 56.4% to 84.3% with an increase in solution pH from 2 to 8. Pseudo-second order kinetic model was found suitable as compared to the pseudo-first order kinetic model. The study revealed that both film diffusion and intraparticle diffusion might have involved in MB adsorption onto CSA. Langmuir isotherm was found best-fit model to describe the equilibrium adsorption with a monolayer adsorption capacity of  $20.42 \text{ mg g}^{-1}$ . The low value (0.201) of separation factor coupled with a negative value of  $\Delta G$  ( $-4.251 \text{ kJ mol}^{-1}$ ) indicated feasible and spontaneous adsorption of MB onto CSA. The present study demonstrated that the CSA could be used as a potential, efficient, low-cost, and easily available adsorbent for the treatment of MB containing industrial wastewater.

## References

- Annadurai, G., Juang, R.S. and Lee, D. J. 2002. Use of cellulose-based wastes for adsorption of dyes from aqueous solutions. *Journal of Hazardous Materials* **B92**: 263-274.
- Arabi, S. and Sohrabi, M.R. 2014. Removal of methylene blue, a basic dye, from aqueous solutions using nano-zerovalent iron. *Water Science and Technology* **70**: 24-31.
- Bharathi, K.S. and Ramesh, S.T. 2013. Removal of dyes using agricultural waste as low-cost adsorbents: a review. *Applied Water Science* **3**: 773-790.
- Feng, Y., Zhou, H., Liu, G., Qiao, J., Wang, J., Lu, H., Yang, L. and Wua, Y. 2012. Methylene blue adsorption onto swede rape straw (*Brassica napus* L.) modified by tartaric acid: Equilibrium, kinetic and adsorption mechanisms. *Bioresource Technology* **125**: 138-144.
- Fiol, N. and I. Villaescusa. 2009. Determination of sorbent point zero charge: usefulness in sorption studies. *Environmental Chemistry Letters* **7**: 79-84.
- Freundlich, H. Z. .1904. Over the adsorption in solution. *The Journal of Physical Chemistry* **5**: 385-470.
- Ghosh, R.K. and Reddy, D.D. 2013. Tobacco stem ash as an adsorbent for removal of methylene blue from aqueous solution: Equilibrium, kinetics and mechanism of adsorption. *Water Air Soil Pollution* **224**(6). DOI: 10.1007/s11270-013-1582-5.
- Ghosh, R.K. and Reddy, D.D. 2014. Crop residue ashes as adsorbents for basic dye (methylene blue) removal: adsorption, kinetics and dynamics. *Clean Soil Air Water* **42**: 1098-1105.
- Hameed, B. H., D. K. Mahmoud, and A. L. Ahmad. 2008. Equilibrium modeling and kinetic studies on the adsorption of basic dye by a low-cost adsorbent: Coconut (*Cocos nucifera*) bunch waste. *Journal of Hazardous Materials* **158**: 65-72.
- Ho, Y. S. and G. McKay. 1998. Sorption of dye from aqueous solution by peat. *Chemical Engineering Journal* **70**: 115-124.
- Jain, A. K., V. K. Gupta, A. Bhatnagar, S. Jain, and Suhas. 2003. A comparative assessment of adsorbents prepared from industrial wastes for the removal of cationic dye. *Journals of Indian Chemical Society* **80**: 267-270.
- Jovanovic, D. S. 1969. Physical adsorption of gases I: isotherms for monolayer and multilayer adsorption. *Colloid and Polymer Science* **235**: 1203-1214.
- Lagergren, S. and B. K. Svenska. 1898. Zur theorie der sogenannten adsorption gelöster stoffe. *Kungl. Svenska vetenskapsakademiens handlingar* **24**: 1-39.
- Lal, R. 2005. World crop residues production and implications of its use as a biofuel. *Environment International* **31**: 575-584.
- Langmuir, I. 1918. The adsorption of gases on plane surfaces of glass, mica, and platinum. *Journal of the American Chemical Society* **40**: 1361-1403.
- Leechart, P., W. Nakbanpote, and P. Thiravetyan. 2009. Application of 'waste' wood-shaving bottom ash for adsorption of azo reactive dye. *Journal of Environmental Management* **90**: 912-920.



- Pathak, B.S. 2006. Crop residues to energy. *Environmental Agriculture* **7**: 854-869.
- Rafatullah, M., Sulaiman, O., Hashim, R. and Ahmad, A. 2010. Adsorption of methylene blue on low cost adsorbents- a review. *Journal of Hazardous Materials* **177**: 70-80.
- Reddy, M.C.S., Sivaramakrishna, L. and Varada Reddy, A. 2012. The use of an agricultural waste material, Jujuba seeds for the removal of anionic dye (Congo red) from aqueous medium. *Journal of Hazardous Materials* **203-204**: 118-127.
- Sarkar, A., Rano, R., Udaybhanu, G. and Basu, A.K. 2006. A comprehensive characterization of fly ash from a thermal power plant in eastern India. *Fuel Processing Technology* **87**: 259-277.
- Sarkar, D. and Bandyopadhyay, A. 2010. Adsorptive mass transport of dye on rice husk ash. *Journal of Water Resource and Protection* **2**: 424-431.
- Temkin, M.J. and Pyzhev, V. 1940. Kinetics of ammonia synthesis on promoted iron catalysts. *Acta physicochimica U.R.S.S.* **12**: 217-222.
- Wang, S. and Zhu, Z.H. 2005. Sonochemical treatment of fly ash for dye removal from wastewater. *Journal of Hazardous Materials* **126**: 91-95.
- Weber Jr, W.J. and Morris, J.C. 1963. Kinetics of adsorption on carbon from solution. *Journal of the Sanitary Engineering Division* **89**: 31-59.
- Weng, C.H. and Pan, Y.F. 2006. Adsorption characteristics of methylene blue from aqueous solution by sludge ash. *Colloids and Surfaces A* **274**: 154-162.
- Yagub, M.T., Sen, T.K. and Ang, H.M. 2012. Equilibrium, kinetics, and thermodynamics of methylene blue adsorption by pine tree leaves. *Water Air Soil Pollution* **223**: 5267-5282.